Proteomic analysis of endocytic vesicles: Rab1a regulates motility of early endocytic vesicles

Aparna Mukhopadhyay[1,2], Edward Nieves[3], Fa-Yun Che[3], Jean Wang[1,2], Lianji Jin[4], John W. Murray[1,2], Kristie Gordon[5], Ruth Hogue Angeletti[4] and Allan W. Wolkoff[1,2,6,*]

[1]Department of Anatomy and Structural Biology, Albert Einstein College of Medicine, Bronx, NY 10461, USA
[2]Marion Bessin Liver Research Center, Albert Einstein College of Medicine, 1300 Morris Park Avenue, Bronx, NY 10461, USA
[3]Laboratory for Macromolecular Analysis and Proteomics, Albert Einstein College of Medicine, Bronx, NY 10461, USA
[4]California State University, 5241 North Maple Avenue, Fresno, CA 93710, USA
[5]Herbert Irving Comprehensive Cancer Center, Columbia University Medical Center, New York, NY 10032, USA
[6]Division of Gastroenterology and Liver Diseases, Albert Einstein College of Medicine, Bronx, NY 10461, USA
*Author for correspondence (allan.wolkoff@einstein.yu.edu)

Accepted 26 October 2010
Journal of Cell Science 124, 765-775
© 2011. Published by The Company of Biologists Ltd
doi:10.1242/jcs.079020

Summary

Texas-Red–asialoorosomucoid (ASOR) fluorescence-sorted early and late endocytic vesicles from rat liver were subjected to proteomic analysis with the aim of identifying functionally important proteins. Several Rab GTPases, including Rab1a, were found. The present study immunolocalized Rab1a to early and late endocytic vesicles and examined its potential role in endocytosis. Huh7 cells with stable knockdown of Rab1a exhibited reduced endocytic processing of ASOR. This correlated with the finding that Rab1a antibody reduced microtubule-based motility of rat-liver-derived early but not late endocytic vesicles in vitro. The inhibitory effect of Rab1a antibody was observed to be specifically towards minus-end-directed motility. Total and minus-end-directed motility was also reduced in early endocytic vesicles prepared from Rab1a-knockdown cells. These results corresponded with virtual absence of the minus-end-directed kinesin Kifc1 from early endocytic vesicles in Rab1a knockdown cells and imply that Rab1a regulates minus-end-directed motility largely by recruiting Kifc1 to early endocytic vesicles.

Key words: Proteomics, Rab1a, Endocytosis

Introduction

Receptor-mediated endocytosis is a process by which ligands that interact with a cell surface receptor are internalized via a clathrin-coated vesicle and undergo a series of processing steps. Soon after internalization, receptor–ligand complexes reside in an early endocytic vesicle that acidifies, resulting in dissociation of the complex. Subsequently, the vesicle undergoes fission, generating a late endocytic vesicle containing most of the ligand and a second daughter vesicle containing most of the receptor that recycles to the cell surface (Bananis et al., 2000; Murray et al., 2008; Pandey, 2009). The late endocytic vesicle targets the ligand to lysosomes for degradation. The liver has an elaborate endocytic machinery responsible for the uptake of various proteins and lipids from the blood, which are subsequently processed and transported to the bile (Schroeder and McNiven, 2009). We have used the hepatocyte-specific asialoglycoprotein receptor (ASGPR) as a prototype of the typical receptor-mediated endocytic pathway (Murray et al., 2008; Murray and Wolkoff, 2003; Shepard et al., 2009; Stockert, 1995). Our previous studies have shown that within 5 minutes of portal venous injection of fluorescent ligand asialoorosomucoid (ASOR) into rat liver, ASOR-containing vesicles are predominantly early endocytic vesicles that mature into late endocytic vesicles by 15 minutes (Bananis et al., 2003; Bananis et al., 2004; Murray et al., 2000). This processing of early endocytic vesicles to late endocytic vesicles requires an intact microtubular cytoskeleton (Gruenberg et al., 1989; Loubery et al., 2008; Soldati and Schliwa, 2006; Wolkoff et al., 1984). In previous studies, we and others identified a number of proteins that are required for endocytic trafficking (Jordens et al., 2001; Murray and Wolkoff, 2005; Murray and Wolkoff, 2007; Nath et al., 2007; Stenmark, 2009). However, it is clear that the endocytic process is complex, and proteins that mediate and regulate activity of this pathway have not yet been elucidated fully.

To discover new endocytic-vesicle-associated proteins, we performed proteomic analysis of rat liver endocytic vesicles loaded in vivo with Alexa-Fluor-488–ASOR and purified by flow cytometry (Bananis et al., 2004). A total of 533 vesicle-associated proteins were identified, some which were found only in early or late vesicles, and some common to both. Several endocytic-vesicle-associated Rab proteins were identified in this study. The Rab proteins are small GTPases that have a regulatory role in many aspects of vesicular transport, including vesicle budding, uncoating, motility and fusion (Somsel Rodman and Wandinger-Ness, 2000; Stenmark, 2009). They function by switching between GDP-bound and GTP-bound states that regulate interactions with other proteins known as effectors. Rab5 has been shown to be involved in the endocytosis of several substrates such as transferrin (Bucci et al., 1992; Nielsen et al., 1999), insulin (Fiory et al., 2004) and the epidermal growth factor receptor (Lanzetti et al., 2000) by regulating motility of early endosomes on microtubules (Nielsen et al., 1999). In studies of early endocytic vesicles containing fluorescent ASOR we found little association with Rab5 but rather association with Rab4 (Bananis et al., 2003). Rab4 has been found to be involved in rapid recycling of transferrin receptors and glycosphingolipids, although the mechanistic function of this protein is unclear (Grant and Donaldson, 2009; van der Sluijs et al., 1992). Late endocytic vesicles contain little Rab4 or Rab5 but instead contain Rab7 (Bananis et al., 2004; Feng et al., 1995), which is also present on lysosomes (Zhang et al., 2009). Such Rab

Journal of Cell Science

conversion has been proposed to be a mechanism by which an early endocytic vesicle matures to a late vesicle (Rink et al., 2005; Rivera-Molina and Novick, 2009) and confers directionality to the pathway.

Rab1a was identified in our proteomics survey to be associated with both early and late endocytic vesicles. The current study aimed to characterize its potential role in endocytosis. There are two isoforms of Rab1, Rab1a and Rab1b, which share 92% amino acid sequence homology (Touchot et al., 1989) and are thought to be functionally redundant in mammalian cells (Tisdale et al., 1992). A role for Rab1 in ER-to-Golgi trafficking has been described previously. Specifically, Rab1 recruits the tethering factor p115 into a *cis*-SNARE complex that programs coat protein II (COPII) vesicles budding from the ER for fusion with the Golgi (Allan et al., 2000) with the help of the *cis*-Golgi tethering protein GM130 complexed to GRASP65 (Moyer et al., 2001). Recently, a role of Rab1a in early-endosome-to-Golgi trafficking has been reported (Sclafani et al., 2010) and Rab1a has been described as a component of transcytotic vesicles (Jin et al., 1996). However, a function for this protein in endocytosis has not been described. In the present study, using siRNA technology to knockdown Rab1a, we studied processing of endocytic vesicles on microtubules in vitro in a reconstituted system (Murray et al., 2000; Murray et al., 2002; Murray and Wolkoff, 2003) and showed that Rab1a is important for transport of early endocytic vesicles along microtubules. Using polarity-marked microtubules, we observed that Rab1a is involved in minus-end-directed motility of early endocytic vesicles. Our previous studies have characterized the motors used in the trafficking of vesicles containing ASOR. Plus-end-directed motility of ASOR-containing early endocytic vesicles prepared from rat and mouse liver is mediated by the conventional kinesin Kif5B (standardized nomenclature, kinesin-1) (Lawrence et al., 2004; Miki et al., 2005; Miki et al., 2003). However, minus-end-directed motility is usually powered by dynein or a small group of minus-end-directed kinesin proteins (Soldati and Schliwa, 2006). Early endocytic vesicles prepared from rat liver use the kinesin motor Kifc2 (Bananis et al., 2003; Bananis et al., 2004), whereas similar vesicles prepared from mouse liver associate with and use the kinesin motor Kifc1 (Nath et al., 2007). Late endocytic vesicles do not use minus-end-directed kinesin motors, but instead use dynein for motility towards the microtubule minus ends (Bananis et al., 2004). In the present study we demonstrate that Rab1a regulates minus-end-directed motility of early endosomes by recruiting the minus-end kinesin Kifc1.

Results

Purification of early and late endocytic vesicles for proteomic analysis

Early and late endocytic vesicles containing Alexa-Fluor-488–ASOR were prepared from rat liver and purified by flow cytometry (Bananis et al., 2004). The presence of markers for early endosomes (the asialoglycoprotein receptor and Rab4) (Bananis et al., 2003) and late endosomes (Rab7 and dynein) (Bananis et al., 2004) were confirmed by immunofluorescence (data not shown). Proteins in each group of endocytic vesicles were resolved on one-dimensional SDS-PAGE and subjected to analysis by nano LC ESI-MS/MS.

Identification and validation of proteins associated with early and late endocytic vesicles

Using the criteria of one or more unique peptide hits each with significant scores ($P<0.05$), 479 proteins were identified in early endocytic vesicles and 271 proteins in late endocytic vesicles. Of these, 217 proteins were common to both early and late vesicles (detailed in supplementary material Tables S1–S3). We identified a number of proteins that are integral membrane proteins or have been implicated in trafficking of membrane proteins, including several Rab GTPases. These selected proteins appear in Tables 1–3. The proteins listed in these tables were identified by virtue of correspondence of two or more significant peptides to the protein sequence.

A group of four proteins consisting of ASGPR, Rab1a, Rab14 and Rab18 that were identified in the purified vesicle preparations were further analyzed. There was substantial colocalization of the Rab proteins with ASOR-containing early and late endocytic vesicles, whereas the ASGPR was largely in early endocytic vesicles (Fig. 1). In this study, we focused on functional aspects of Rab1a in endocytic trafficking. As seen in Fig. 1, 52% (n=290) of early and 36% (n=591) of late endocytic vesicles containing ASOR were associated with Rab1a. Conversely, only 6% (n=4297) of Rab1a-containing vesicles colocalized with ASOR.

Early endocytic vesicles associated with Rab1a do not bind p115

Mass spectrometric analysis also identified p115 as one of the components of early endocytic vesicles. As this was not a quantitative survey, additional studies were performed. To validate the presence of p115 and determine its importance in endocytosis, early endocytic vesicles were immunostained for p115 in addition to Rab1a using specific antibodies and colocalization was quantified. Although vesicles positive for both p115 and Rab1a were seen [52% of the Rab1a vesicles (n=2213) contained p115, Fig. 2A], because the endosomal preparation contained other organellar membranes, including those from the Golgi and ER, few (6%, n=194) endocytic vesicles containing Texas-Red–ASOR colocalized with p115. Interestingly, 84% (n=194) of the ASOR vesicles containing Rab1a excluded p115, indicating that in endosomes containing Rab1a, p115 is unlikely to be an effector.

Rab1a-associated early endocytic vesicles are also associated with Rab4

Our previous studies showed that 80% of ASOR-containing early endocytic vesicles are associated with Rab4 (Bananis et al., 2003). By contrast, late endocytic vesicles contain little Rab4 but are instead associated with Rab7 (Bananis et al., 2004). We examined the distribution of Rab4 in Rab1a-positive ASOR-containing early endocytic vesicles using Rab4-specific antibody in addition to anti-Rab1a. These studies revealed that 86% (n=954) of the Rab1a-containing early endosomes were also associated with Rab4 (Fig. 2B) but only 44% of Rab4-containing early endocytic vesicles were also associated with Rab1a.

siRNA knockdown of Rab1a

To investigate a role for Rab1a in endocytic vesicle trafficking, studies were performed in the human hepatoma cell line Huh7 in which Rab1a expression was knocked down using siRNA technology. These cells express the asialoglycoprotein receptor and have been used in a number of previous studies of endocytic trafficking (Huang et al., 2002; Stockert et al., 2007; Treichel et al., 1994). In case Rab1a knockdown proved toxic to the cells, a Tet-inducible system was chosen that required the preparation of a cell line expressing Tet repressor (TR).

Plasmids containing the siRNA target sequence of Rab1a were transfected into the TR cell line and stable clones were selected and picked in the presence of puromycin. These cell lines were called 223 and 372, which refers to the nucleotide in the coding region of Rab1a used as target sequence for knockdown. A control cell line (PS) was also created by transfection with the empty pSuperior vector. siRNA was induced in each of the clones in the presence of 0.1 μg/ml doxycycline and lysates were immunoblotted for Rab1a. As a control, lysates from uninduced cells were used. It was observed that even in the absence of doxycycline induction, there was no detectable expression of Rab1a in the clones containing the siRNA sequences (Fig. 3A). These results implied

Table 1. Selected proteins identified in early but not late endocytic vesicles[a]

Protein name	Accession No.	Mass (Da)	% Coverage	No. of unique peptides
Annexin A2	Q07936	38,523	7.1	3
Annexin A5	P14668	35,591	11	2
Annexin A6	P48037	75,575	9.2	4
Clathrin light chain A	P08081	26,964	6	2
General vesicular transport factor p115	P41542	107,096	10.7	6
Low affinity immunoglobulin gamma Fc region receptor II precursor	Q63203	32,027	23.9	5
Lysosome membrane protein II[b]	P27615	53,925	6.5	4
Myosin Ib[b]	Q05096	131,835	2.5	2
PDZ domain-containing protein 1	Q9JJ40	56,765	8.8	3
Ras-related protein Rab1B	P10536	22,149	31.3	3
Ras-related protein Rab18[b]	Q5EB77	22,962	5.3	3
Ras-related protein Rab1b precursor[b]	Q62636	20,785	6	2
Single Ig IL-1-related receptor	Q4V892	46,142	22.2	5
Sodium/potassium-transporting ATPase β1 chain[b]	P07340	35,179	8.2	3
Solute carrier organic anion transporter family member 1A1	P46720	74,129	12.2	3
Solute carrier organic anion transporter family member 1A4[b]	O35913	73,203	3.3	7
Solute carrier organic anion transporter family member 1B2[b]	Q9QZX8	72,719	2	3
Solute carrier organic anion transporter family member 2B1	Q9JHI3	74,166	3.5	2
Sulfate anion transporter 1	P45380	75,399	7.7	3
Vesicle-associated membrane protein-associated protein A	Q9Z270	27,206	11.6	2
Vimentin	P31000	53,569	35.9	12

[a]Selected proteins of interest each containing at least two significant peptides in early and late endocytic vesicles. Mass, molecular mass of protein (Dalton); % Coverage, percentage coverage of the peptides of the whole protein. [b]Proteins listed in both early and late vesicles but in late vesicles only one significant peptide was identified.

Table 2. Selected proteins identified in late but not early endocytic vesicles[a]

Protein name	Accession No.	Mass (Da)	% Coverage	No. of unique peptides
Long-chain fatty acid CoA ligase 6	P33124	78,130	3.4	2
Tubulin α6 chain	Q6AYZ1	49,905	8	2
Vesicle-associated membrane protein 8	Q9WUF4	11,313	24	2

[a]Selected proteins of interest each containing at least two significant peptides in early and late endocytic vesicles.

Table 3. Selected proteins identified in both early and late endocytic vesicles[a]

			% Coverage		No. of unique peptides	
Protein name	Accession No.	Mass (Da)	EV	LV	EV	LV
Asialoglycoprotein receptor 1	P02706	32,697	25.8	21.2	7	6
MRP2	Q63120	173,274	9.9	3.3	6	2
Clathrin heavy chain	P11442	191,477	30.6	15.8	40	10
Golgin subfamily A member 5	Q3ZU82	82,284	22.1	7.7	10	3
Myosin-9	Q62812	226,066	41.3	35	62	51
Polymeric-immunoglobulin receptor precursor	P15083	84,745	29.8	8.6	17	4
Ras-related protein Rab11A	P62494	24,247	35.3	19.1	6	3
Ras-related protein Rab14	P61107	23,912	25.1	12.1	3	2
Ras-related protein Rab1A	Q6NYB7	22,532	34.8	41.2	5	5
Ras-related protein Rab2A	P05712	23521	19.3	14.2	3	2
Ras-related protein Rab6A	Q9WVB1	15,763	37.9	37.9	4	2
Ras-related protein Rab7	P09527	23,489	21.7	28	3	5
Serotransferrin precursor	P12346	76,314	40	11.2	20	6
Sodium/potassium-transporting ATPase α1 chain precursor	P06685	112,982	20.9	8.9	18	5
Syntaxin-7	O70257	29,643	11.5	8.1	2	2
Transferrin receptor protein 1	Q99376	70,109	17.5	11.4	10	5

[a]Selected proteins of interest each containing at least two significant peptides in early and late endocytic vesicles. EV, early vesicles; LV, late vesicles.

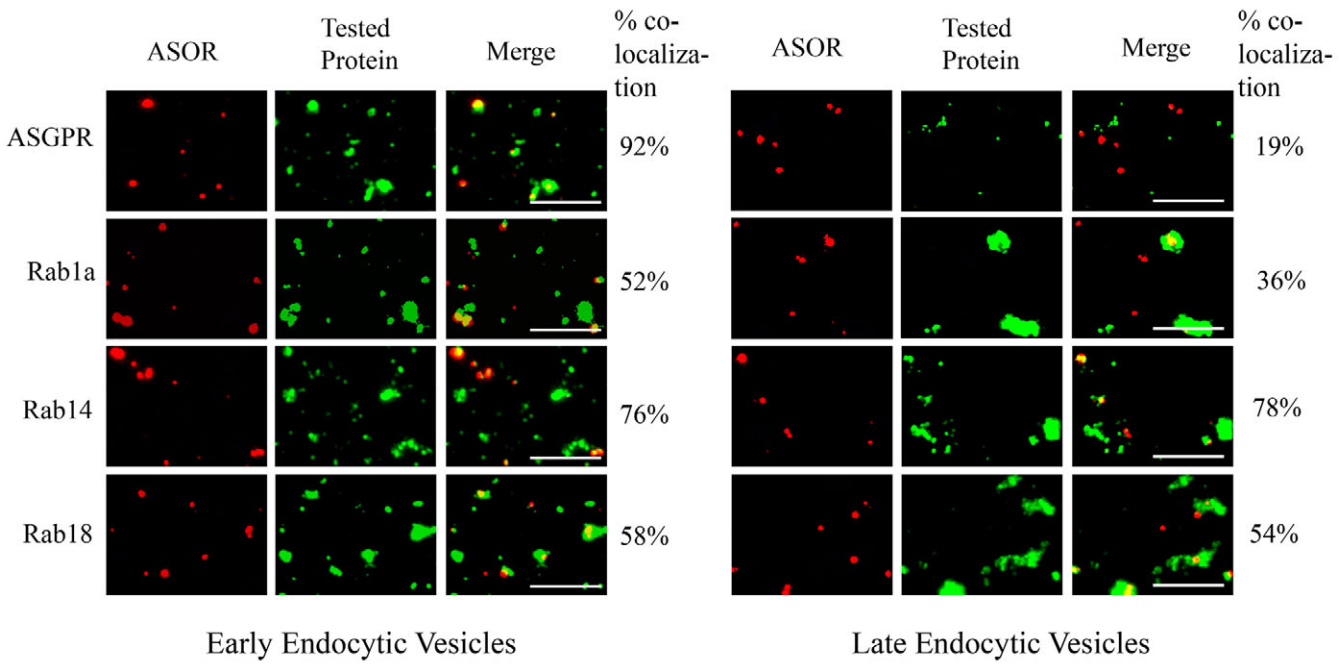

Fig. 1. Validation of proteins identified by proteomic analysis of FACS purified early and late endocytic vesicles. Texas-Red–ASOR-containing early (left panel) and late (right panel) endocytic vesicles were stained for selected proteins as indicated using specific antibodies. The images were pseudocolored and merged using ImageJ. Colocalization was quantified and is indicated as a percentage of vesicles containing ASOR. Scale bars: 10 μm.

that the Tet-inducible system was leaky, but growth and morphologic appearance of the Rab1a knockdown (KD) cells were the same as those of PS and Huh7 cells. Consequently, these cells were used for further studies in the absence of doxycycline treatment. Expression of Rab1b and Rab4 in these cells was unchanged (Fig. 3B), indicating specific knockdown of Rab1a.

Golgi and ER morphology is normal in Rab1a KD cells

As Rab1a has been described as a protein involved in ER-Golgi trafficking, we examined whether its knockdown would affect the appearance of these organelles. As seen in Fig. 3C, morphology of the Golgi (p115, in green) and ER (PDI, in red) in the two Rab1a KD cell lines did not differ from the empty vector (PS) cell line.

ASOR trafficking is perturbed in Rab1a KD cells

To test the role of Rab1a in endocytic trafficking in cultured cells, live-cell imaging following fluorescent ASOR uptake in Rab1a KD cells was performed. Fig. 4A is a composite panel of representative images, showing time-dependent accumulation of fluorescence as vesicles containing endocytosed fluorescent ligand grow larger and brighter in the Rab1a KD cells in contrast to the control PS cells. Images from three independent experiments were quantified where the maximum and minimum pixel intensity values of all the images were set and the mean pixel intensity of individual cells measured by ImageJ. To normalize values between experiments and different cell lines, the pixel intensity at time 0 was set at 1 and the values of the other time points calculated accordingly. These data, represented graphically in Fig. 4B, show the increase in pixel intensity of fluorescence in the Rab1a KD cells, indicating accumulation of protein. By contrast, the PS cells did not get brighter over time, indicating that endocytosed ASOR is efficiently processed and degraded in these cells.

To determine directly whether there is a defect in intracellular ASOR processing in Rab1a KD cells, surface binding and degradation of [^{125}I]ASOR was assayed. In these studies, [^{125}I]ASOR was bound to the surface of cells at 4°C, excess was washed away and the cells were shifted to 37°C to initiate endocytosis. Normally, endocytosed ASOR is delivered to lysosomes for degradation. Degraded protein is quantified through measurement of acid soluble radioactivity in the medium, whereas surface bound ligand is estimated from radioactivity released with 20 mM EGTA. In the control PS cells, we observed that 34% of [^{125}I]ASOR that had been bound to the cell surface at time 0 was degraded by 90 minutes (Fig. 4C). Degradation was significantly reduced in the Rab1a KD cell line 223 to 18% of that initially bound to the surface (P<0.02), consistent with impaired delivery of ligand to lysosomes in the absence of Rab1a. Because all experiments with the two Rab1a KD cell lines yielded similar results, data from further experiments using the two cell lines were combined and are represented as Rab1a KD. Similarly, results of Huh7 and PS were combined as a control because both of these cell lines yielded identical results.

Rab1a antibody reduces microtubule-based motility of early but not late endocytic vesicles

Previously, we showed that early and late endocytic vesicles can attach to and move along microtubules in vitro (Bananis et al., 2000; Bananis et al., 2003; Bananis et al., 2004; Murray et al., 2000; Murray et al., 2002; Murray et al., 2008; Murray and Wolkoff, 2005; Murray and Wolkoff, 2007) and this trafficking is an essential part of the endocytic processing of ASOR (Novikoff et al., 1996). Slower processing (Fig. 4B) and reduced degradation (Fig. 4C) of ASOR in the absence of Rab1a could be due to reduced motility of vesicles as they traffic via microtubules to reach lysosomes. Initial experiments examined the effect of Rab1a antibody preincubation on motility of

Journal of Cell Science

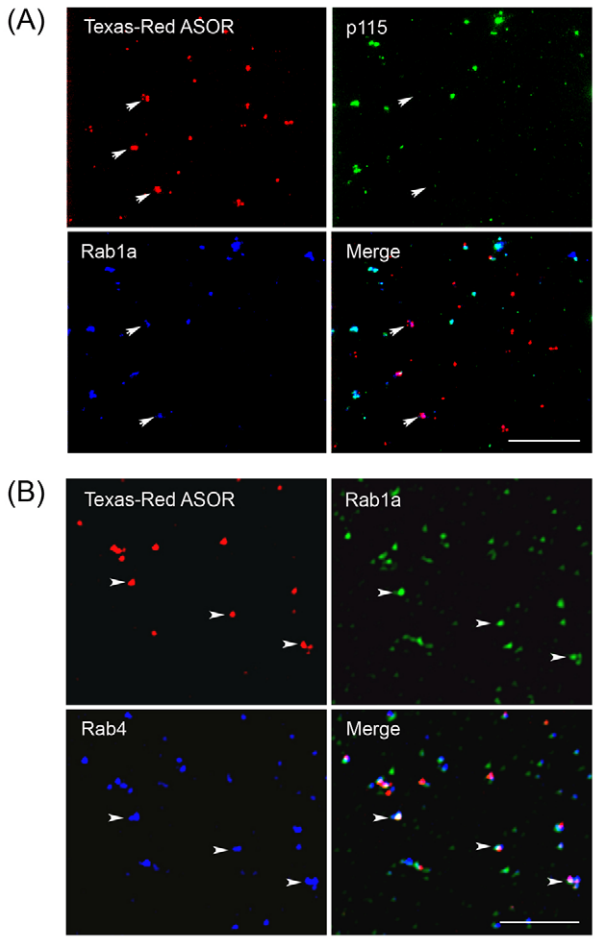

Fig. 2. Texas-Red–ASOR-containing early endocytic vesicles that colocalize with Rab1a contain Rab4 but not p115. Texas-Red–ASOR-containing early endocytic vesicles were stained for Rab1a and either p115 (**A**) or Rab4 (**B**) using specific antibodies. Images were pseudocolored and merged using Image J. Arrows in A indicate vesicles containing Rab1a and Texas Red, but excluding p115. Arrows in B indicate vesicles containing Texas Red, Rab1a and Rab4. Scale bars: 10 µm.

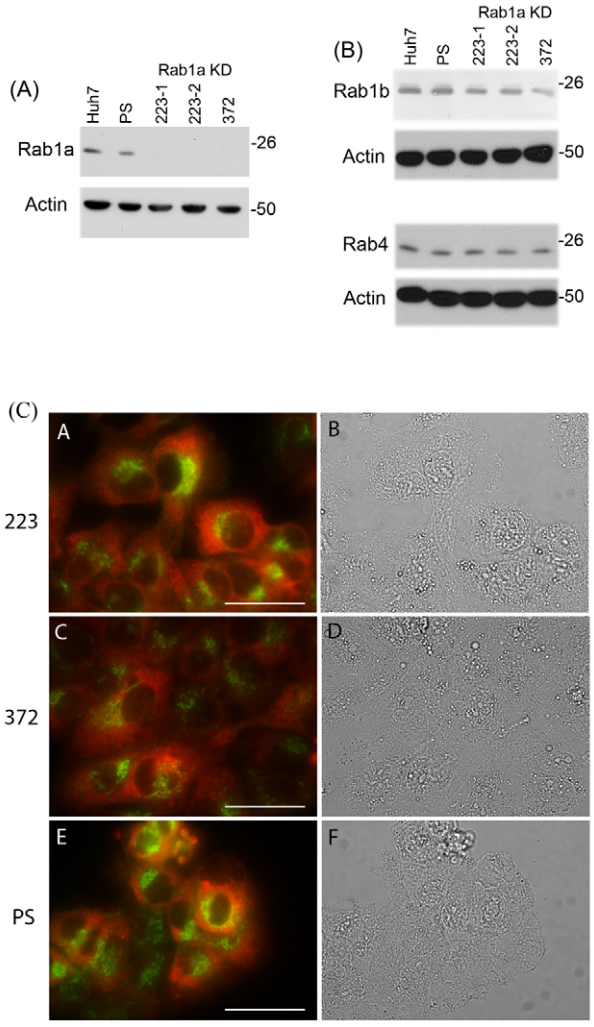

Fig. 3. SiRNA knockdown of Rab1a. Huh7 cells were stably transfected with siRNA designed to knockdown Rab1a. (**A**,**B**) Lysates from parental Huh7, empty pSuperior transfected (PS) cell lines and those from different clones from the two Rab1a KD cells lines, 223 and 372 (Rab1a KD) were subjected to immunoblotting for Rab1a (A), Rab1b or Rab4 (B) as indicated. The gels were also probed for actin as a loading control. Position of molecular size markers (in kDa) is indicated. (**C**) ER and Golgi morphology in Rab1a KD cells. Rab1a KD cell lines, 223 and 372 as well as control (PS) cells were grown on MatTek plates and stained for the Golgi marker p115 (green) and the ER marker PDI (red). Single channel images were merged and pseudocolored using ImageJ software. Panels on the right represent the bright-field images of panels to the left. Scale bars: 50 µm.

endocytic vesicles on microtubules. In these studies, motility of endocytic vesicles containing Texas-Red–ASOR on microtubules was assayed following preincubation of vesicles with anti-Rab1a antibody. Control studies were performed in the absence of antibody and in the presence of nonimmune rabbit IgG. In the absence of antibody, 44% (n=318) of early endocytic vesicles on microtubules were motile (Fig. 5A). By contrast, only 25% (n=303, P<0.001) of early endocytic vesicles moved on microtubules following preincubation with Rab1a antibody. This was not due to a non-specific effect of IgG, because motility of these vesicles was enhanced in the presence of non-immune IgG (Fig. 5A). Interestingly, there was no effect on the motility of late endocytic vesicles upon preincubation with Rab1a antibody (Fig. 5A).

Early endocytic vesicles prepared from Rab1a KD cells have reduced microtubule-based motility

To further establish a role for Rab1a in microtubule-based motility, we prepared early endocytic vesicles containing Alexa-Fluor-488–ASOR from the Rab1a KD and control cells and used them in motility assays similar to that described above. Of these vesicles prepared from control and KD cells, 70% contained the ASGPR receptor as assessed by immunostaining, indicating that they are largely early endocytic vesicles (data not shown). As seen in Fig. 5B, in the absence of Rab1a, fewer (30–35%, P<0.001) vesicles moved on microtubules compared with those prepared from the control PS cells (51%). A representative movie of motility of vesicles prepared from Huh7 cells is shown in supplementary material Movie 1.

Rab1a is required for minus-end-directed movement of early endocytic vesicles on microtubules

The studies presented above show that Rab1a is required for optimal motility of early endocytic vesicles on microtubules. In

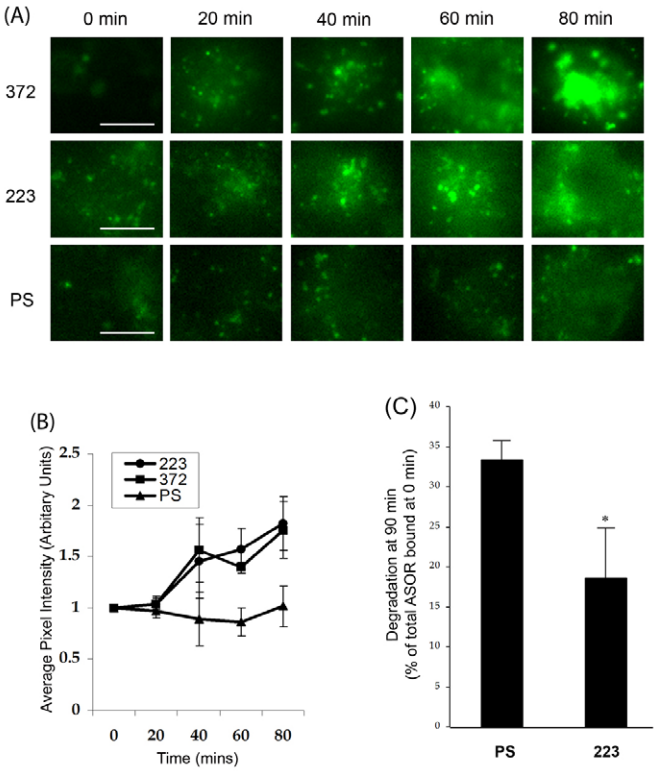

Fig. 4. Rab1a KD cells exhibit impaired processing and degradation of ASOR. The Rab1a KD cell lines (223 and 372) as well as the vector-transfected control cells (PS) were grown on MatTek plates and were used for a study where uptake of Alexa-Fluor-488–ASOR prebound to the cell surface was followed for 80 minutes (min) by live-cell imaging. (**A**) Representative images. For clarity in print, the brightness and contrast of these images were enhanced beyond the adjustments described in B. Scale bar: 5 μm. (**B**) Graphical representation of average pixel intensity of Alexa-Fluor-488–ASOR in cells over 80 minutes. Pixel intensities of all images from three independent experiments were set to the same maximum and minimum level and the mean gray value of individual cells were measured using ImageJ. To normalize between different cell lines and experiments, the value at 0 minutes was set at 1.0 and all other values calculated accordingly by dividing the mean intensity at each time point with the mean intensity at time 0 minutes. Error bars represent s.d. from the mean. (**C**) Degradation of [^{125}I]ASOR in Rab1a KD (223) and control (PS) cells. [^{125}I]ASOR was initially bound to cells on ice and then allowed to be taken up by endocytosis by shifting the cells to 37°C. Degraded ASOR was measured by counting acid soluble radioactivity in the medium at the end of 90 minutes. In replicate plates, surface-bound ASOR at 0 minutes was released in 20 mM EGTA and counted. Degradation at 90 minutes was calculated as a percentage of the total amount of ASOR that was surface bound at 0 minutes. Error bars represent s.d. *P<0.02.

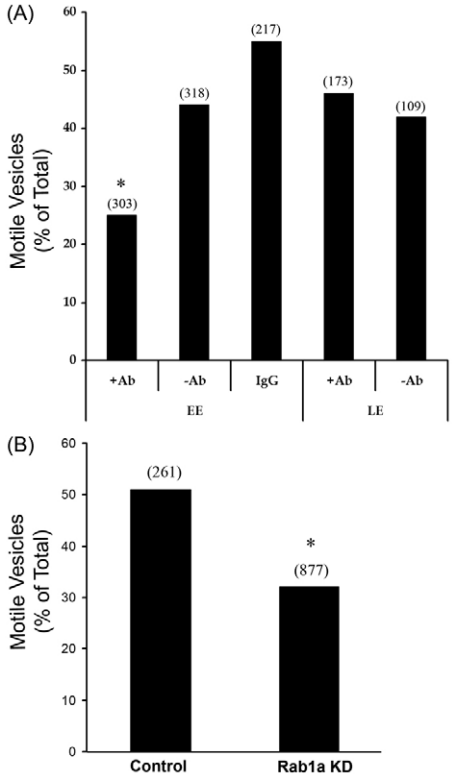

Fig. 5. Rab1a regulates motility of early endocytic vesicles on microtubules. (**A**) Texas-Red–ASOR-containing early (EE) and late (LE) endocytic vesicles were attached to Rhodamine-labeled microtubules and their motility in the presence (+Ab) or absence (–Ab) of Rab1a antibody was studied. A control experiment was performed in the presence of normal rabbit IgG (IgG). (**B**) Motility of early endocytic vesicles prepared from Rab1a KD (223 and 372) and control cells (PS and Huh7). The percentage of microtubule-bound vesicles that moved upon addition of 50 μM ATP is shown. In both panels, the number of total vesicles counted is in parentheses. *P<0.001.

further studies, we examined whether all movement was reduced or whether there was a specific reduction in movement towards the plus or minus ends of microtubules. To examine this question, motility assays were performed with polarity-marked microtubules and the number of vesicles moving towards the plus and the minus ends were quantified. An example of vesicle motility on polarity marked microtubules is shown in supplementary material Movie 2. Similarly to previous results (Bananis et al., 2000), it was observed that almost equal numbers of early endocytic vesicles moved towards the plus and minus ends (27% and 30% of total vesicles, respectively, Fig. 6A). Upon preincubation with Rab1a antibody, plus-end-directed motility remained the same (32%), but minus-end-directed motility diminished significantly (11% of total vesicles, P<0.001). To further establish a requirement for Rab1a in minus-end-directed motility, we used early endocytic vesicles from Rab1a KD cells and quantified their directional motility. Similarly to results in the presence of Rab1a antibody, the vesicles from Rab1a KD cells had reduced motility (12% of total vesicles, P<0.001) towards the minus end of microtubules when compared with the control (28% of total vesicles, Fig. 6B).

Rab1a regulates minus-end-directed motility of early endocytic vesicles by recruiting Kifc1

A defect in minus-end-directed motility of vesicles lacking Rab1a indicated that activity of a minus-end-directed motor could be regulated by Rab1a. Our previous work has characterized the plus and minus end motors driving motility of endocytic vesicles derived from rat and mouse livers (Bananis et al., 2000; Bananis et al., 2003; Bananis et al., 2004; Murray et al., 2000; Murray and Wolkoff, 2003; Nath et al., 2007). As the Rab1a KD cells are derived from the human hepatoma cell line Huh7, we examined which minus-end-directed motor is used by these vesicles, because they were previously uncharacterized. Early endocytic vesicles containing Alexa-Fluor-488–ASOR were prepared from the Rab1a KD and control cell lines and immunostained for dynein, Kifc1

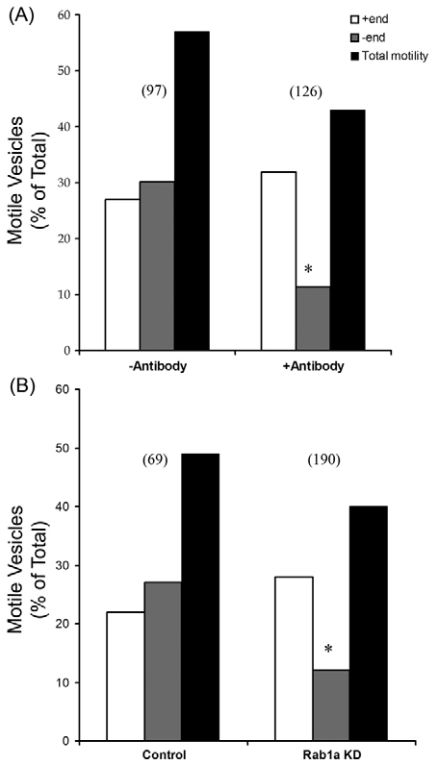

Fig. 6. Rab1a regulates minus-end-directed motility of early endocytic vesicles. Polarity marked microtubules were prepared and motility of (**A**) Texas-Red–ASOR-containing early endocytic vesicles in the presence (+Ab) and absence (–Ab) of Rab1a antibody and (**B**) Alexa-Fluor-488–ASOR-containing vesicles prepared from the Rab1a KD (223 and 372) and control cells (PS and Huh7) were studied. The percentage of total vesicles moving towards the plus and minus ends was scored and is represented graphically. The numbers in parentheses indicate the total number of vesicles attached to polarity marked microtubules that were counted. **P*<0.001.

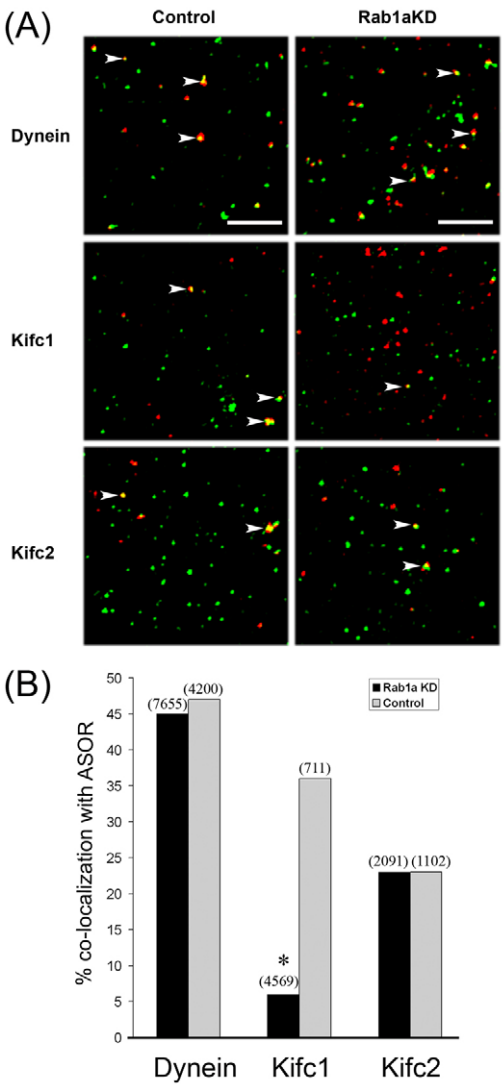

Fig. 7. Rab1a recruits the minus-end-directed kinesin motor Kifc1 to early endocytic vesicles. Alexa-Fluor-488–ASOR-containing early endocytic vesicle were prepared from Rab1a KD (223 and 372) and control PS cells and stained with antibody against dynein, Kifc1 or Kifc2. (**A**) A panel of representative images showing colocalization of early endocytic vesicles from the cell lines with the indicated motor proteins. Arrowheads indicate ASOR-containing vesicles colocalizing with the indicated motor protein. Scale bars: 10 μm. (**B**) Graphical representation of the percentage colocalization. Rab1a KD, black bars; PS, gray bars. The numbers in parentheses indicate the total number of vesicles examined. **P*<0.001.

and Kifc2 using specific antibodies (Fig. 7A). Represented graphically in Fig. 7B is a quantification of the amount of colocalization observed between the motor proteins with Alexa-Fluor-488–ASOR. Among the vesicles prepared from the control cells, 47% colocalized with dynein, 36% with Kifc1 and 23% with Kifc2. Similar numbers of vesicles prepared from the Rab1a KD cells colocalized with dynein (45%) and Kifc2 (23%). Interestingly however, these vesicles exhibited an almost complete lack of colocalization (6%, $P<0.001$) with Kifc1. These data indicate that Rab1a is essential for the recruitment of Kifc1 to early endocytic vesicles.

Discussion

In the present study, fluorescent ASOR-containing early and late endocytic vesicles were highly enriched using fluorescence sorting and subjected to proteomic analysis. A number of transporters and potential regulatory molecules were identified. The presence of the organic anion transporters, transferrin receptor, polymeric immunoglobulin receptor, asialoglycoprotein receptor and Na^+/K^+-transporting ATPase in the early endocytic vesicles indicate that many proteins that are endocytosed from the cell surface use the same vesicle, at least initially. It has been observed previously that 45% of ASOR vesicles colocalize with the bile acid transporter, Na^+-taurocholate co-transporting polypeptide (NTCP) and 65% of the NTCP vesicles colocalize with transferrin receptor (Sarkar et al., 2006), indicating that a population of NTCP and transferrin could possibly use the same pathway as ASOR for uptake from the cell surface. ASGPR1 and clathrin (Murray and Wolkoff, 2003; Stockert, 1995; Wolkoff et al., 1984), which are known to be present exclusively in early endosomes, were also identified in late endocytic vesicles. This could be due to partial contamination of late endocytic vesicles with early vesicles, because preparation of vesicles involves the injection of fluorescent ASOR into the portal vein of rats, which, despite high first-pass extraction, still exhibits a component of non-synchronous uptake into the liver.

Journal of Cell Science

Several potential regulatory molecules such as annexin-2, annexin-5 and annexin-6, syntaxin-7 and Rab1a, Rab1b, Rab2A, Rab6A, Rab7, Rab8B, Rab11A, Rab14 and Rab18 were also detected. The Rab proteins that have been described to have a role in various stages of endocytic trafficking are Rab4, Rab5, Rab7, Rab9, Rab15 and Rab22 (Stenmark, 2009), and this study reveals a previously unknown function of Rab1a in this process. Previously we reported that 80–90% of Texas-Red–ASOR-containing early endocytic vesicles prepared from rat liver contain Rab4 (Bananis et al., 2003). In the present study, we show that a similar percentage of ASOR vesicles associated with Rab1a also contained Rab4. However, only 44% of ASOR vesicles containing Rab4 were associated with Rab1a. This could indicate that Rab4 associates with early endocytic vesicles before Rab1a and might be involved in the recruitment of Rab1a to these vesicles. There are several reports that describe possible mechanisms of how multiple Rab proteins function and coordinate with each other on the same vesicle (Del Conte-Zerial et al., 2008; Fukuda et al., 2008; Markgraf et al., 2007; Rivera-Molina and Novick, 2009; Sonnichsen et al., 2000; Spang, 2009).

Rab1 has been implicated in regulation of COPII vesicle fusion to the *cis*-Golgi in association with p115, GM130 and GRASP65 (Allan et al., 2000; Moyer et al., 2001). Rab1a has also been described as a component in the transcytotic pathway in rat liver (Jin et al., 1996). This pathway traffics cargo such as polymeric IgA (pIgA) and its receptors from the basolateral hepatocyte membrane to the apical side where vesicle content is released into the bile canaliculus. These pIgA-rich transcytotic vesicles are also associated with p115 (Jin et al., 1996; Sztul et al., 1991) and both the polymeric immunoglobulin receptor and p115 were discovered to be components of early endocytic vesicles. In the present study, we report the presence of vesicles that contain endocytosed ASOR that colocalize with Rab1a, but exclude p115 (Fig. 2A). These data show that Rab1a can associate with specific vesicles in the absence of p115, indicating that Rab1a uses different effectors to function simultaneously in regulating endocytosis as well as ER-to-Golgi trafficking.

Knockdown Huh7 cell lines were created for examination of the role of Rab1a in endocytosis. These cell lines expressed Rab1b and Rab4 and exhibited normal morphology of the Golgi and ER. There are mixed reports on the effect of Rab1a knockdown on the Golgi. Transient transfections into HeLa and HEK293 cells resulted in complete fragmentation of the Golgi in some reports (Hyvola et al., 2006; Razi et al., 2009; Winslow et al., 2010), whereas less or no fragmentation in others (Dejgaard et al., 2008; Dumaresq-Doiron et al., 2010). Our studies differ from these reports because we created stable cell lines with knockdown of Rab1a, in contrast to the use of transfected siRNAs. The simplest explanation for lack of any fragmentation in our cells is compensation of the loss of Rab1a by Rab1b because both isoforms have redundant functions although there are several ways a cell could adapt itself, which would be manifested only in a stable cell line. Dysfunction of the secretory pathway cannot be ruled out, although it would probably be minor considering the normal appearance and growth of these cells.

The knockdown cell lines exhibited slower processing and degradation of the endocytic ligand ASOR, implying that Rab1a is involved in endocytic processing of ASOR. Because vesicle maturation and endocytic processing require trafficking of vesicles on microtubules, in vitro analysis of vesicle movement on microtubules was examined. The use of an inhibitory antibody against Rab1a in vesicle-motility assays revealed reduced motility of early but not late endocytic vesicles. This suggests that Rab1a has an important role in the processing of early endocytic vesicles. Although a significant number (36%) of late endocytic vesicles also contain Rab1a, it does not appear to be involved in motility of these vesicles on microtubules. Studies using vesicles prepared from Rab1a KD cells confirmed that Rab1a influences the trafficking of early endocytic vesicles on microtubules. Hence the slower processing and reduced degradation of ASOR observed in these cells could be attributed to reduced motility of vesicles that allowed ASOR to accumulate in the cells.

Experiments using polarity-marked microtubules showed that anti-Rab1a antibody specifically inhibits minus-end-directed motility of vesicles on microtubules. A role for Rab1a in minus-end-directed motility was confirmed using vesicles lacking Rab1a that were prepared from Huh7 cells lines with a stable knockdown of Rab1a. This effect of Rab1a is topologically significant, because movement of vesicles from the cell surface to lysosomes requires trafficking towards the minus end of microtubules.

Minus-end-directed motility is potentially driven by two motors: cytoplasmic dynein and C-terminal minus-end-directed kinesins, which are members of the kinesin-14 family (Soldati and Schliwa, 2006). Among the minus-end-directed kinesins, only Kifc1 (kinesin-14A), Kifc2 (kinesin-14B) and Kifc3 have been reported to be involved in intracellular trafficking (Nath et al., 2007; Xu et al., 2002; Yang and Sperry, 2003; Yang and Goldstein, 1998; Yang et al., 2001). Our previous studies showed that ASOR-containing early endocytic vesicles prepared from rat liver use Kifc2 (Bananis et al., 2000; Bananis et al., 2003; Bananis et al., 2004; Murray et al., 2000), whereas those prepared from mouse livers use Kifc1 (Nath et al., 2007) for minus-end-directed motility. Although a substantial number of ASOR-containing vesicles colocalize with NTCP, the NTCP vesicles use dynein for minus-end-directed motility (Sarkar et al., 2006). In the present study, immunofluorescence experiments using ASOR-containing early endocytic vesicles prepared from parental Huh7 cells showed 47% colocalization with dynein, 35% with Kifc1 and 23% with Kifc2. The presence of dynein in these vesicles is in contrast to our earlier observations using early endocytic vesicles from rat and mouse liver. This could represent differences in timing of endocytic processing between cell lines and intact liver. The minimal colocalization of Kifc1 with ASOR-containing vesicles prepared from Rab1a KD cells indicates that Rab1a is required for the recruitment of the motor Kifc1 to these endocytic vesicles. This provides an explanation for the loss of minus-end-directed motility in vesicles lacking Rab1a.

This study indicates that although Rab1a is present in both early and late endocytic vesicles, it is required for motility of only early endocytic vesicles towards the minus end of microtubules by the recruitment of Kifc1. We hypothesize that Rab1a functions as a scaffold to which stage-specific proteins and motors can bind. This represents a novel function of Rab1a, which is distinct from its well-characterized function in the secretory pathway.

Materials and Methods

Cells, reagents and antibodies

The human hepatoma cell line Huh7 was maintained in RPMI medium containing L-glutamine (Mediatech, Manassas, VA) and supplemented with 10% fetal bovine serum (Atlanta Biologicals, Lawrenceville, GA) and 1% penicillin-streptomycin (Mediatech). For the tetracycline-inducible system, Tet System approved serum was purchased from Clontech Laboratories, Mountain View, CA. Tris(2-carboxyethyl)phosphine hydrochloride (TCEP) was purchased from Pierce, Rockford, IL. Trifluoroacetic acid (TFA, protein sequencer grade) was from Applied Biosystems,

Journal of Cell Science

Foster City, CA. All other reagents were from Sigma-Aldrich, St Louis, MO, unless otherwise noted. All chemicals were of analytical grade or higher.

The following antibodies were used: rabbit polyclonal antibodies against Rab1a, Rab1b, Dynein and normal rabbit IgG were purchased from Santa Cruz Biotechnology (Santa Cruz, CA); mouse anti-Rab4 (BD Transduction Laboratories, San Jose, CA); rabbit polyclonal anti-Rab14 (Abcam, Cambridge, MA); rabbit polyclonal anti-Rab18 (Calbiochem, San Diego, CA); mouse p115 (a gift from Dennis Shields, Albert Einstein College of Medicine, NY); rabbit anti-PDI (Stressgen, Ann Arbor, MI); mouse anti-β-actin (Sigma); mouse anti-human Kifc1 (AbD Serotec, Oxford, UK); rabbit polyclonal anti Kifc2 (Nath et al., 2007); Cy5-conjugated Goat Anti-Rabbit IgG and Cy3-conjugated goat anti-mouse IgG (H+L) (Jackson ImmunoResearch Laboratories, West Grove, PA).

Preparation of labeled ASOR

Asialoorosomucoid (ASOR) was prepared by hydrolysis of human α_1-orosomucoid (Sigma) in 0.1 N sulfuric acid at 75°C for 1 hour. The solution was neutralized with 1 N NaOH, dialyzed against water, and protein concentration determined as described previously (Stockert et al., 1995). Fluorescent ASOR was prepared by conjugation with either Texas Red sulfonyl chloride or Alexa Fluor 488 carboxylic acid, succinimidyl ester (Molecular Probes, Eugene, OR) following the manufacturer's instructions. [^{125}I]ASOR was prepared by incubating 100 μg ASOR with 5 mCi $Na^{125}I$ (Perkin Elmer, Boston, MA) in the presence of Pierce iodination beads (Pierce Biotechnology, Rockford, IL) for 15 minutes. The solution was applied to a 20 ml G25 column and radioactivity in 0.5 ml fractions was determined in a gamma counter. The early fractions containing maximum radioactivity were pooled and used for uptake studies. A yield of 400–600 c.p.m./ng ASOR was usually achieved.

Preparation of early and late endocytic vesicles

Fluorescent ASOR containing early and late endocytic vesicles were prepared from livers of 200–250 g male Sprague–Dawley rats (Taconic Farms, Germantown, NY) as described previously (Bananis et al., 2003). Briefly, livers were removed either 5 minutes (for early endocytic vesicles) or 15 minutes (for late endocytic vesicles) after injection of 50 μg Texas-Red–ASOR into the portal vein. After Dounce homogenization, a postnuclear supernatant was obtained which was then subjected to Sephacryl S200 (Pharmacia, Uppsala, Sweden) column chromatography. Vesicle enriched fractions (cloudy fractions) were pooled and adjusted to 1.4 M sucrose. This was then layered at the bottom of a 1.4–1.2–0.25 M discontinuous sucrose density gradient and subjected to centrifugation at 100,000 ***g*** for 2 hours. The vesicles were harvested from the 1.2–0.25 M sucrose interface and stored in small aliquots at –80°C until used. All animal procedures were approved by the Animal Institute Committee of the Albert Einstein College of Medicine.

Early endocytic vesicles were also prepared from Huh7 cells. The cells were incubated on ice with 1.5 μg/ml Alexa-Fluor-488–ASOR in buffer (135 mM NaCl, 0.81 mM $MgSO_4$, 1.2 mM $MgCl_2$, 27.8 mM glucose, 2.5 mM $CaCl_2$, 25 mM HEPES, pH 7.2) for 1 hour. Unbound ASOR was removed by washing and the cells were incubated at 37°C for 7 minutes to initiate endocytosis. The cells were then washed in cold buffer, lysed by Dounce homogenization and vesicles were prepared similarly to those from rat livers, the only difference being omission of the Sephacryl S200 column chromatography step.

Flow cytometric purification of fluorescent early and late endocytic vesicles

Alexa-Fluor-488–ASOR-containing endocytic vesicles were subjected to sorting on a DakoCytomation Modular Flow (MoFlo) High-Performance Cell Sorter (DakoCytomation, Fort Collins, CO) equipped with a 488 nm coherent argon laser and a collection/emission 530/540 nm filter. For control determinations, unlabeled vesicles were isolated from rat livers that had not been injected with ASOR. Data acquisition and analysis was performed using DakoCytomation MoFlo Summit Software (DakoCytomation, Fort Collins, CO). Details and validation of this procedure have been published (Bananis et al., 2004).

Proteomic analysis of vesicle-associated proteins

Following fluorescence sorting, approximately 3×10^8 early or late endocytic vesicles (70–90 μg protein) were subjected to SDS-PAGE separation using 10% polyacrylamide precast minigels (Bio-Rad, Hercules, CA). Approximately 10–15 μg of vesicle protein in sample buffer was applied to each of six lanes on separate gels for early and late vesicles. Protein was visualized following staining for 10–15 minutes with 0.2% Coomassie Blue. Each lane was then cut into approximately 50 sequential slices of ~1 mm thickness. Corresponding slices from each of the lanes were combined, cut into 1×1 mm pieces, and washed with water. The gel pieces were destained in 0.2 M NH_4HCO_3, pH 8.9 and acetonitrile (1:1 v/v) and reduced in 0.1 M NH_4HCO_3, pH 8.9 containing 10 mM DTT at 56°C. The reduced cysteine residues were subsequently alkylated in 55 mM iodoacetamide in 100 mM NH_4HCO_3 and the gel pieces were then washed in acetonitrile and dried. The dried gel pieces were treated with approximately 200 ng trypsin (sequencing grade; Promega, Madison, WI) in 50 mM NH_4HCO_3, pH 8.9 on ice for 45 minutes, the excess removed and the digestion was allowed to complete at 37°C for 18 hours in 50 mM NH_4HCO_3, pH 8.9. Trifluoroacetic acid (TFA) was then added to a final concentration of 0.1% and used for nano LC ESI-MS/MS analysis.

Nanoelectrospray LC-MS/MS analysis and protein identification

Tryptic digests were loaded and separated using the UltiMate FAMOS Switchos nano-HPLC system (LC Packings, Dionex; Sunnyvale, CA) connected online to a LTQ Linear Ion Trap mass spectrometer (Thermo Fisher Scientific, Waltham, MA) equipped with a nanospray source. The mobile phases consisted of 5% acetonitrile in water, 0.1% formic acid (A) and 80% acetonitrile in water, 0.1% formic acid (B). After injection (15 μl sample) and loading onto a C_{18} trap column, 0.3 mm ID ×5 mm, the tryptic peptides were separated on a C_{18} analytical HPLC column (75 μm ID ×15 cm; Pepmap, 3 μm, 100 A; LC Packings, Dionex, Sunnyvale, CA). The flow rate for loading and desalting was 15 μl/minute for 30 minutes and the analytical separation was performed at 250 nl/minute. The gradient used was: 2% to 55% B over 65 minutes; hold at 55% B for 10 minutes; increase to 95% B for 5 minutes and hold at 95% B for another 5 minutes. The HPLC eluent was electrosprayed into the LTQ using the nanospray source. After an initial MS survey scan, *m/z* 300–1800, MS/MS scans were obtained from the three most intense ions using a normalized collision energy of 35%. DTA files were generated from the raw data files, merged and searched against the SwissProt *Rattus* database with Mascot (version 2.1.04). The search parameters used were: variable modifications – N/Q deamidation, oxidized Met, carbamidomethyl C; 1 missed cleavage; peptide mass tolerance of ±2 Da and ±0.8 Da for product ions.

Immunoblot analysis

Immunoblots were performed as we have described previously (Bananis et al., 2004). In brief, presorted endocytic vesicles were subjected to SDS-PAGE (~15 μg total protein/lane) under reducing conditions (100 mM DTT) and transferred to a PVDF membrane (Perkin Elmer, Boston, MA). The membrane was blocked with TBS (50 mM Tris-HCl, 150 mM NaCl, pH 7.6) containing 0.1% Tween 20 and 10% nonfat dried milk before incubation with primary antibody diluted appropriately in TBS, 0.1% Tween 20 and 2% nonfat dried milk. Immunoblot analysis was then performed using appropriate primary and HRP-conjugated secondary antibodies.

Immunofluorescence and motility assay of vesicles

Immunofluorescence and microtubule-based vesicle motility studies were performed in an optical chamber as described previously (Murray et al., 2002; Murray and Wolkoff, 2007). Vesicles were stained for selected proteins using specific antibodies in buffer containing 35 mM PIPES-K_2, 5 mM $MgCl_2$, 1 mM EGTA, 0.5 mM EDTA, 2 mg/ml BSA, 4 mM DTT, 2 mg/ml vitamin C with 5 mg/ml casein, pH 7.4.

Fluorescent microtubules were polymerized from a 7:1 mixture of tubulin (10 mg/ml) and Rhodamine–tubulin (1.7 mg/ml) (Cytoskeleton Inc., Denver, CO) in buffer containing 8 mM PIPES-K_2, 1 mM EGTA, 1 mM $MgCl_2$, 1 mM GTP with 3% glycerol, pH 7.0 at 37°C. The polymerized microtubules were stabilized and stored in this buffer supplemented with 20 μM Taxol. In experiments involving polarity marked microtubules, end labeling was achieved by initially polymerizing 'dim' seeds containing unlabeled and Rhodamine–tubulin at a ratio of 72:1 for 5 minutes. These seeds were sheared and 'bright' tubulin that had unlabeled and rhodamine tubulin at a concentration of 6:1 in the buffer described above was added and allowed to polymerize for 6 minutes. The polarity marked microtubules were stored in 20 μM Taxol-containing buffer and used the same day.

For motility experiments, microtubules were diluted in MT buffer (35 mM PIPES-K_2, 5 mM $MgCl_2$, 1 mM EGTA, 0.5 mM EDTA, 2 mg/ml BSA, pH 7.4 with 20 μM Taxol) and flowed into an optical chamber that had been precoated with 30 μg/ml DEAE-dextran. After washing off excess microtubules, vesicles were flowed in and allowed to bind to the microtubules at room temperature for 10 minutes in a humidified chamber. In experiments involving addition of Rab1a antibody, vesicles were washed in blocking buffer (35 mM PIPES-K_2, 5 mM $MgCl_2$, 1 mM EGTA, 0.5 mM EDTA, 2 mg/ml BSA, 4 mM DTT, 2 mg/ml vitamin C with 5 mg/ml casein, pH 7.4) before addition of antibody diluted 1:50 in the same buffer. Upon completion of antibody incubation, the chamber was washed in assay buffer (35 mM PIPES-K_2, 5 mM $MgCl_2$, 1 mM EGTA, 0.5 mM EDTA, 2 mg/ml BSA, 4 mM DTT, 2 mg/ml vitamin C, pH 7.4). Images were acquired upon addition of 50 μM ATP to the optical chamber on the microscope stage heated to 37°C.

siRNA knockdown of Rab1a

A stable Huh7 cell line expressing the Tet Repressor was established by transfection of pcDNA6/TR (Invitrogen, Carlsbad, CA) and selecting stable clones in 1.5 μg/ml blasticidine S HCl (Invitrogen, Carlsbad, CA). Individual clones were selected and tested for expression of Tet repressor by immunoblotting using Tet repressor antibody (MoBitec, Goettingen). The clone expressing the highest level of Tet Repressor was used subsequently.

Rab1a was knocked down by siRNA using a vector-based approach. Two target sequences were selected 5′-CAATCACCTCCAGTTATTA-3′ and 5′-CAAATGTGATCTGACCACA-3′ corresponding to nucleotides 223 and 372 in the human *RAB1A* sequence (Accession No. NM_004161). Oligonucleotides containing the sense-loop-antisense sequence were synthesized and cloned into pSuperior.Puro (Oligoengine, Seattle, WA) following the manufacturer's instructions. The vectors were transfected into Huh7 cells expressing Tet repressor (TR cells). Stable clones were selected in 2.0 μg/ml puromycin (Clontech, Mountain View, CA). Individual clones were selected and tested for Rab1a expression by immunoblotting in the absence or presence of 0.1 μg/ml doxycycline hyclate (Sigma). Clones exhibiting

maximum knockdown of Rab1a expression were selected and used for subsequent studies.

ASOR-uptake studies

For fluorescent ASOR-uptake studies, cells were grown to confluence either on 50 mm MatTek plates (MatTek Corporation, Ashland, MA) or eight-well Labtek chambers (Thermo Fisher Scientific, Rochester, NY). The plates were chilled on ice and 10 μg/ml Alexa-Fluor-488–ASOR in binding buffer (135 mM NaCl, 0.81 mM $MgSO_4$, 1.2 mM $MgCl_2$, 27.8 mM glucose, 2.5 mM $CaCl_2$, 25 mM HEPES, pH 7.2) was added and allowed to bind for 1 hour on ice. Excess unbound ASOR was removed by washing and the plates were warmed to 37°C on the microscope stage, and images were captured over 90 minutes.

[^{125}I]ASOR-uptake assays were performed as described previously (Stockert et al., 2007). Briefly, cells were grown to confluence and chilled on ice before addition of 1.2 μg [^{125}I]ASOR per plate in binding buffer. In control plates, 100 μg of unlabeled ASOR was added to estimate non-specific binding. ASOR was allowed to bind for 1 hour on ice and the excess washed off before the plates were shifted to 37°C to initiate endocytosis. Degradation was estimated by counting acid (10% trichloroacetic acid, 2% phosphotungstic acid) soluble radioactivity in the medium, whereas surface-bound ASOR was released in 20 mM EGTA and counted.

Image acquisition and processing

Images were acquired with a 60× 1.4 numerical aperture Olympus objective on an Olympus 1×71 inverted microscope containing automated excitation and emission filter wheels maintained at 37°C. Data were collected through a CoolSNAP HQ cooled charge-coupled device (Photometrics, Roper Scientific, Tucson, AZ) camera regulated by MetaMorph (Molecular Devices, Sunnyvale, CA) software. Fluorescent images were analyzed using ImageJ 1.39u (National Institutes of Health public domain; rsb.info.nih.gov/ij/) and Adobe Photoshop CS2 version 9.0.2 (Adobe Systems, San Jose, CA).

Colocalization of fluorescent vesicles was automatically quantified using the Autoscore_Co-localization macro written by John W. Murray to run in ImageJ 1.39u software. This macro is based on previous methods (Murray et al., 2002) and functions by segmenting images of vesicles into discrete spots and quantifying the presence of fluorescence at each spot in images of alternate fluorescence channels of the same field. It uses the SpotEnhancing filter written by Daniel Sage (Biomedical Imaging Group, Lausanne, Switzerland) and the Analyze Particles function of ImageJ 1.39u. Threshold intensity is chosen automatically based on image intensity and standard deviation.

For microtubule-based motility studies, time-lapse movies were taken at 1 frame per second for 90 seconds. Movies were analyzed using ImageJ 1.39u software by scoring the number of vesicles on microtubules and manually counting those that exhibited movement. Vesicles were considered motile if they were observed to move from their original position along a microtubule over a span of two or more frames. Vesicles that were not on microtubules or those that flowed away upon addition of ATP were not scored. In experiments involving use of polarity marked microtubules, only those vesicles on microtubules where the polarity could be distinguished were scored.

Live cell fluorescent ASOR uptake images at different time points were first normalized by setting the maximum and minimum pixel intensity values within the same limits using ImageJ 1.39u. The mean gray value of individual cells was measured and an average calculated for each time point. In order to normalize the intensity of fluorescence between different cell lines, the intensity was set at 1.0 for time 0 minutes and that of all the other time points were calculated accordingly by dividing the mean intensity value at each time point by the intensity value at time 0 minutes.

Statistical analysis

Statistical analysis was performed using Chi-square or Student's *t*-test as appropriate using Microsoft Excel 2000.

This work was supported by National Institutes of Health grants DK41918, DK07218 and DK041296. Deposited in PMC for release after 12 months.

Supplementary material available online at
http://jcs.biologists.org/cgi/content/full/124/5/765/DC1

References

Allan, B. B., Moyer, B. D. and Balch, W. E. (2000). Rab1 recruitment of p115 into a cis-SNARE complex: programming budding COPII vesicles for fusion. *Science* **289**, 444-448.

Bananis, E., Murray, J. W., Stockert, R. J., Satir, P. and Wolkoff, A. W. (2000). Microtubule and motor-dependent endocytic vesicle sorting in vitro. *J. Cell Biol.* **151**, 179-186.

Bananis, E., Murray, J. W., Stockert, R. J., Satir, P. and Wolkoff, A. W. (2003). Regulation of early endocytic vesicle motility and fission in a reconstituted system. *J. Cell Sci.* **116**, 2749-2761.

Bananis, E., Nath, S., Gordon, K., Satir, P., Stockert, R. J., Murray, J. W. and Wolkoff, A. W. (2004). Microtubule-dependent movement of late endocytic vesicles in vitro: requirements for Dynein and Kinesin. *Mol. Biol. Cell* **15**, 3688-3697.

Bucci, C., Parton, R. G., Mather, I. H., Stunnenberg, H., Simons, K., Hoflack, B. and Zerial, M. (1992). The small GTPase rab5 functions as a regulatory factor in the early endocytic pathway. *Cell* **70**, 715-728.

Dejgaard, S. Y., Murshid, A., Erman, A., Kizilay, O., Verbich, D., Lodge, R., Dejgaard, K., Ly-Hartig, T. B., Pepperkok, R., Simpson, J. C. et al. (2008). Rab18 and Rab43 have key roles in ER-Golgi trafficking. *J. Cell Sci.* **121**, 2768-2781.

Del Conte-Zerial, P., Brusch, L., Rink, J. C., Collinet, C., Kalaidzidis, Y., Zerial, M. and Deutsch, A. (2008). Membrane identity and GTPase cascades regulated by toggle and cut-out switches. *Mol. Syst. Biol.* **4**, 206.

Dumaresq-Doiron, K., Savard, M. F., Akam, S., Costantino, S. and Lefrancois, S. (2010). The phosphatidylinositol 4-kinase PI4KIIIalpha is required for the recruitment of GBF1 to Golgi membranes. *J. Cell Sci.* **123**, 2273-2280.

Feng, Y., Press, B. and Wandinger-Ness, A. (1995). Rab **7**, an important regulator of late endocytic membrane traffic. *J. Cell Biol.* **131**, 1435-1452.

Fiory, F., Oriente, F., Miele, C., Romano, C., Trencia, A., Alberobello, A. T., Esposito, I., Valentino, R., Beguinot, F. and Formisano, P. (2004). Protein kinase C-ζ and protein kinase B regulate distinct steps of insulin endocytosis and intracellular sorting. *J. Biol. Chem.* **279**, 11137-11145.

Fukuda, M., Kanno, E., Ishibashi, K. and Itoh, T. (2008). Large scale screening for novel rab effectors reveals unexpected broad Rab binding specificity. *Mol. Cell. Proteomics* **7**, 1031-1042.

Grant, B. D. and Donaldson, J. G. (2009). Pathways and mechanisms of endocytic recycling. *Nat. Rev. Mol. Cell Biol.* **10**, 597-608.

Gruenberg, J., Griffiths, G. and Howell, K. E. (1989). Characterization of the early endosome and putative endocytic carrier vesicles in vivo and with an assay of vesicle fusion in vitro. *J. Cell Biol.* **108**, 1301-1316.

Huang, T., Deng, H., Wolkoff, A. W. and Stockert, R. J. (2002). Phosphorylation-dependent interaction of the asialoglycoprotein receptor with molecular chaperones. *J. Biol. Chem.* **277**, 37798-37803.

Hyvola, N., Diao, A., McKenzie, E., Skippen, A., Cockcroft, S. and Lowe, M. (2006). Membrane targeting and activation of the Lowe syndrome protein OCRL1 by rab GTPases. *EMBO J.* **25**, 3750-3761.

Jin, M., Saucan, L., Farquhar, M. G. and Palade, G. E. (1996). Rab1a and multiple other Rab proteins are associated with the transcytotic pathway in rat liver. *J. Biol. Chem.* **271**, 30105-30113.

Jordens, I., Fernandez-Borja, M., Marsman, M., Dusseljee, S., Janssen, L., Calafat, J., Janssen, H., Wubbolts, R. and Neefjes, J. (2001). The Rab7 effector protein RILP controls lysosomal transport by inducing the recruitment of dynein-dynactin motors. *Curr. Biol.* **11**, 1680-1685.

Lanzetti, L., Rybin, V., Malabarba, M. G., Christoforidis, S., Scita, G., Zerial, M. and Di Fiore, P. P. (2000). The Eps8 protein coordinates EGF receptor signalling through Rac and trafficking through Rab5. *Nature* **408**, 374-377.

Lawrence, C. J., Dawe, R. K., Christie, K. R., Cleveland, D. W., Dawson, S. C., Endow, S. A., Goldstein, L. S., Goodson, H. V., Hirokawa, N., Howard, J. et al. (2004). A standardized kinesin nomenclature. *J. Cell Biol.* **167**, 19-22.

Loubery, S., Wilhelm, C., Hurbain, I., Neveu, S., Louvard, D. and Coudrier, E. (2008). Different microtubule motors move early and late endocytic compartments. *Traffic* **9**, 492-509.

Markgraf, D. F., Peplowska, K. and Ungermann, C. (2007). Rab cascades and tethering factors in the endomembrane system. *FEBS Lett.* **581**, 2125-2130.

Miki, H., Setou, M. and Hirokawa, N. (2003). Kinesin superfamily proteins (KIFs) in the mouse transcriptome. *Genome Res.* **13**, 1455-1465.

Miki, H., Okada, Y. and Hirokawa, N. (2005). Analysis of the kinesin superfamily: insights into structure and function. *Trends Cell Biol.* **15**, 467-476.

Moyer, B. D., Allan, B. B. and Balch, W. E. (2001). Rab1 interaction with a GM130 effector complex regulates COPII vesicle cis-Golgi tethering. *Traffic* **2**, 268-276.

Murray, J. W. and Wolkoff, A. W. (2003). Roles of the cytoskeleton and motor proteins in endocytic sorting. *Adv. Drug Deliv. Rev.* **55**, 1385-1403.

Murray, J. W. and Wolkoff, A. W. (2005). Assay of Rab4-dependent trafficking on microtubules. *Methods Enzymol.* **403**, 92-107.

Murray, J. W. and Wolkoff, A. W. (2007). In vitro motility system to study the role of motor proteins in receptor-ligand sorting. *Methods Mol. Biol.* **392**, 143-158.

Murray, J. W., Bananis, E. and Wolkoff, A. W. (2000). Reconstitution of ATP-dependent movement of endocytic vesicles along microtubules in vitro: an oscillatory bidirectional process. *Mol. Biol. Cell* **11**, 419-433.

Murray, J. W., Bananis, E. and Wolkoff, A. W. (2002). Immunofluorescence microchamber technique for characterizing isolated organelles. *Anal. Biochem.* **305**, 55-67.

Murray, J. W., Sarkar, S. and Wolkoff, A. W. (2008). Single vesicle analysis of endocytic fission on microtubules in vitro. *Traffic* **9**, 833-847.

Nath, S., Bananis, E., Sarkar, S., Stockert, R. J., Sperry, A. O., Murray, J. W. and Wolkoff, A. W. (2007). Kif5B and Kifc1 interact and are required for motility and fission of early endocytic vesicles in mouse liver. *Mol. Biol. Cell* **18**, 1839-1849.

Nielsen, E., Severin, F., Backer, J. M., Hyman, A. A. and Zerial, M. (1999). Rab5 regulates motility of early endosomes on microtubules. *Nat. Cell Biol.* **1**, 376-382.

Novikoff, P. M., Cammer, M., Tao, L., Oda, H., Stockert, R. J., Wolkoff, A. W. and Satir, P. (1996). Three-dimensional organization of rat hepatocyte cytoskeleton: relation to the asialoglycoprotein endocytosis pathway. *J. Cell Sci.* **109**, 21-32.

Journal of Cell Science

Pandey, K. N. (2009). Functional roles of short sequence motifs in the endocytosis of membrane receptors. *Front. Biosci.* **14**, 5339-5360.
Razi, M., Chan, E. Y. W. and Tooze, S. A. (2009). Early endosomes and endosomal coatomer are required for autophagy. *J. Cell Biol.* **185**, 305-321.
Rink, J., Ghigo, E., Kalaidzidis, Y. and Zerial, M. (2005). Rab conversion as a mechanism of progression from early to late endosomes. *Cell* **122**, 735-749.
Rivera-Molina, F. E. and Novick, P. J. (2009). A Rab GAP cascade defines the boundary between two Rab GTPases on the secretory pathway. *Proc. Natl. Acad. Sci. USA* **106**, 14408-14413.
Sarkar, S., Bananis, E., Nath, S., Anwer, M. S., Wolkoff, A. W. and Murray, J. W. (2006). PKCzeta is required for microtubule-based motility of vesicles containing the ntcp transporter. *Traffic* **7**, 1078-1091.
Schroeder, B. and McNiven, M. (2009). *Endocytosis as an Essential Process in Liver Function and Pathology.* Chichester, West Sussex: Wiley-Blackwell.
Sclafani, A., Chen, S., Rivera-Molina, F., Reinisch, K., Novick, P. and Ferro-Novick, S. (2010). Establishing a role for the GTPase Ypt1p at the late golgi. *Traffic* **11**, 520-532.
Shepard, B. D., Fernandez, D. J. and Tuma, P. L. (2009). Alcohol consumption impairs hepatic protein trafficking: mechanisms and consequences. *Genes Nutr*. (Epub ahead of print).
Soldati, T. and Schliwa, M. (2006). Powering membrane traffic in endocytosis and recycling. *Nat. Rev Mol. Cell Biol.* **7**, 897-908.
Somsel Rodman, J. and Wandinger-Ness, A. (2000). Rab GTPases coordinate endocytosis. *J. Cell Sci.* **113**, 183-192.
Sonnichsen, B., De Renzis, S., Nielsen, E., Rietdorf, J. and Zerial, M. (2000). Distinct membrane domains on endosomes in the recycling pathway visualized by multicolor imaging of Rab4, Rab5, and Rab11. *J. Cell Biol.* **149**, 901-914.
Spang, A. (2009). On the fate of early endosomes. *Biol. Chem.* **390**, 753-759.
Stenmark, H. (2009). Rab GTPases as coordinators of vesicle traffic. *Nat. Rev. Mol. Cell Biol.* **10**, 513-525.
Stockert, R. J. (1995). The asialoglycoprotein receptor: relationships between structure, function, and expression. *Physiol. Rev.* **75**, 591-609.
Stockert, R. J., Potvin, B., Tao, L., Stanley, P. and Wolkoff, A. W. (1995). Human hepatoma cell mutant defective in cell surface protein trafficking. *J. Biol. Chem.* **270**, 16107-16113.
Stockert, R. J., Potvin, B., Nath, S., Wolkoff, A. W. and Stanley, P. (2007). New liver cell mutants defective in the endocytic pathway. *Biochim. Biophys. Acta* **1768**, 1741-1749.
Sztul, E., Kaplin, A., Saucan, L. and Palade, G. (1991). Protein traffic between distinct plasma membrane domains: isolation and characterization of vesicular carriers involved in transcytosis. *Cell* **64**, 81-89.
Tisdale, E. J., Bourne, J. R., Khosravi-Far, R., Der, C. J. and Balch, W. E. (1992). GTP-binding mutants of rab1 and rab2 are potent inhibitors of vesicular transport from the endoplasmic reticulum to the Golgi complex. *J. Cell Biol.* **119**, 749-761.
Touchot, N., Zahraoui, A., Vielh, E. and Tavitian, A. (1989). Biochemical properties of the YPT-related rab1B protein. Comparison with rab1A. *FEBS Lett.* **256**, 79-84.
Treichel, U., Meyer zum Buschenfelde, K. H., Stockert, R. J., Poralla, T. and Gerken, G. (1994). The asialoglycoprotein receptor mediates hepatic binding and uptake of natural hepatitis B virus particles derived from viraemic carriers. *J. Gen. Virol.* **75**, 3021-3029.
van der Sluijs, P., Hull, M., Webster, P., Male, P., Goud, B. and Mellman, I. (1992). The small GTP-binding protein rab4 controls an early sorting event on the endocytic pathway. *Cell* **70**, 729-740.
Winslow, A. R., Chen, C. W., Corrochano, S., Acevedo-Arozena, A., Gordon, D. E., Peden, A. A., Lichtenberg, M., Menzies, F. M., Ravikumar, B., Imarisio, S. et al. (2010). alpha-Synuclein impairs macroautophagy: implications for Parkinson's disease. *J. Cell Biol.* **190**, 1023-1037.
Wolkoff, A. W., Klausner, R. D., Ashwell, G. and Harford, J. (1984). Intracellular segregation of asialoglycoproteins and their receptor: a prelysosomal event subsequent to dissociation of the ligand-receptor complex. *J. Cell Biol.* **98**, 375-381.
Xu, Y., Takeda, S., Nakata, T., Noda, Y., Tanaka, Y. and Hirokawa, N. (2002). Role of KIFC3 motor protein in Golgi positioning and integration. *J. Cell Biol.* **158**, 293-303.
Yang, W. X. and Sperry, A. O. (2003). C-terminal kinesin motor KIFC1 participates in acrosome biogenesis and vesicle transport. *Biol. Reprod.* **69**, 1719-1729.
Yang, Z. and Goldstein, L. S. (1998). Characterization of the KIF3C neural kinesin-like motor from mouse. *Mol. Biol. Cell* **9**, 249-261.
Yang, Z., Roberts, E. A. and Goldstein, L. S. (2001). Functional analysis of mouse C-terminal kinesin motor KifC2. *Mol. Cell. Biol.* **21**, 2463-2466.
Zhang, M., Chen, L., Wang, S. and Wang, T. (2009). Rab7: roles in membrane trafficking and disease. *Biosci. Rep.* **29**, 193-209.

Journal of Cell Science